https://doi.org/10.5194/acp-2021-444
Preprint. Discussion started: 1 July 2021

Atmospheric Chemistry and Physics Discussions

Dynamical evolution of a minor sudden stratospheric warming in the Southern Hemisphere in 2019

Guangyu Liu[1], Toshihiko Hirooka[1], Nawo Eguchi[2] and Kirstin Krüger[3]

[1]Department of Earth and Planetary Sciences, Kyushu University, Fukuoka, Japan
[2]Research Institute for Applied Mechanics, Kyushu University, Kasuga, Japan
[3]Department of Geosciences, University of Oslo, Oslo, Norway

Correspondence to: Nawo Eguchi (nawo@riam.kyushu-u.ac.jp), Guangyu Liu (liu.guangyu.465@m.kyushu-u.ac.jp)

Abstract.

This study analyzes the Japanese 55-year Reanalysis (JRA-55) dataset from 2002 to 2019 to examine the sudden stratospheric warming event that occurred in the Southern Hemisphere (SH) in 2019 (hereafter referred to as SSW2019). Strong warming at the polar cap and decelerated westerly winds were observed, but since there was no reversal of westerly winds to easterly winds at 60°S in the middle to lower stratosphere, the SSW2019 is classified as a minor warming event.

The results show that quasi-stationary planetary waves of zonal wavenumber 1 developed during the SSW2019. The strong vertical component of the Eliassen–Palm flux with zonal wavenumber 1 is indicative of pronounced propagation of planetary waves to the stratosphere. The wave driving in September 2019 shows that the values are larger than those of the major SSW event in 2002 (hereafter referred to as SSW2002). Since there was no pronounced preconditioning (as in SSW2002) and the polar vortex was already strong before the SSW2019 occurred, a major disturbance of the polar vortex was unlikely to have taken place. The strong wave driving in SSW2019 occurred in high latitudes. Waveguides (i.e., positive values of the refractive index) are found at high latitudes in the upper stratosphere during the warming period, which provided favorable conditions for quasi-stationary planetary waves to propagate upward and poleward.

1 Introduction

Sudden stratospheric warmings (hereafter referred to as SSWs) are extraordinary events that are regularly observed in the Arctic polar region during winter. Strong westerly winds associate with the polar vortex in the mid-to-high latitudes decelerate, and temperatures increase by several tens of Kelvins within a few days in the polar region during a SSW (Labitzke and van Loon, 1999; Andrews et al., 1987; Iida et al., 2014; Baldwin et al., 2021). Many studies have examined the underlying mechanisms of these events. SSWs are caused by enhanced quasi-stationary planetary waves that propagate from the troposphere to the stratosphere (Matsuno, 1971). The occurrence of SSWs is common in the Northern Hemisphere (NH) (Charlton and Polvani, 2007) but rare in the Southern Hemisphere (SH) (Roscoe et al., 2005; Naujokat and Roscoe, 2005) due to the relatively weak wave activity there resulting from the ocean–land distribution and small wave perturbations (Andrews et al., 1987).

https://doi.org/10.5194/acp-2021-444
Preprint. Discussion started: 1 July 2021

Atmospheric Chemistry and Physics Discussions

SSWs during mid-winter are classified as either major or minor warmings (Julian, 1967; Labitzke, 1968). Major warming events are defined by rapid temperature increases between 60° latitude and the pole, and a breakdown of the polar vortex, where zonal-mean zonal winds at 10 hPa poleward of 60° latitude reverse from westerly to easterly. In contrast, minor warming events refer to high temperatures at the pole without a reversal of zonal-mean zonal winds poleward of 60° latitude at 10 hPa. Moreover, major warmings can be classified as being of the "vortex-displacement" or "vortex-split" type depending on the structure of the polar vortex during the onset of the warming event (Charlton and Polvani, 2007). Planetary waves with zonal wavenumbers 1 and 2 (PW1, PW2) play an important role in the preconditioning of the polar vortex (Labitzke, 1981; Bancalá et al., 2012).

In the SH, minor warming events have occasionally been observed in mid-winter (i.e., Godson 1963; Labitzke and van Loon 1965; Barnett 1974; Al-Ajmi et all., 1985; Hirota et al., 1990; Shiotani et al., 1993), whilst only one major SSW event has been detected in 2002 (Roscoe et al., 2005; Naujokat and Roscoe, 2005). Before the onset of SSW2002, a sequence of amplified planetary-wave activity was observed, which played an important role in weakening the polar night jet (PNJ) (Krüger et al., 2005). Then, the polar vortex broke down in September and split into two. The strong eastward-traveling waves, consisting primarily of PW2, led to wave-mean flow interactions that weakened the PNJ, whilst the amplified quasi-stationary waves caused the disruption of the polar vortex and abruptly increased the polar temperature. The SSW2002 was classified as a major warming event of the "vortex-split" type applying the criteria of Charlton and Polvani (2007). The SSW2002 in the SH also significantly impacted the interannual variability of the Antarctic ozone hole (Weber et al., 2003). The warm air and particularly strong wave activity during SSW2002 disrupted the depletion of ozone over Antarctica, leading to the smallest ozone hole since 1988 (Allen et al., 2003; Newman and Nash, 2005; Stolarski et al., 2005).

In September 2019, a strong SSW occurred in the SH (Yamazaki et al., 2020; Hendon et al., 2019; Eswaraiah et al., 2020). Rao et al. (2020) investigated the predictability of an SSW event that occurred in the SH in 2019 based on subseasonal to seasonal (S2S) models and identified favorable conditions such as easterly equatorial quasi-biennial oscillation (QBO) winds at 10 hPa, solar minimum, and positive Indian Ocean Dipole (IOD) sea surface temperatures that may have led to its occurrence. Following SSW2019, a significant reduction of the ozone hole area was detected during the peak ozone depletion period based on the Aura Microwave Limb Sounder (MLS) of Aura satellite and Global Earth Observing System model simulations (Wargan et al., 2020). Safieddine et al. (2020) showed that the total ozone poleward of 45°S increased during September to November 2019 using the Infrared Atmospheric Sounding Interferometer.

The purpose of this study is to investigate the dynamical evolution of the SSW2019 and compare it with the SSW2002 event in the SH. The data and analysis methods are described in Sect. 2, followed by a discussion of the evolution and

https://doi.org/10.5194/acp-2021-444
Preprint. Discussion started: 1 July 2021

dynamical features of SSW2019 in Sect. 3. Section 4 discusses the plausible factors that may have contributed to the occurrence of SSW2019. A summary and conclusion are presented in Sect. 5.

2 Data and Analysis Methods

2.1 The JRA-55 reanalysis data

This study used horizontal winds, temperature, and geopotential height from the Japanese 55-year Reanalysis (JRA-55) dataset provided by the Japan Meteorological Agency. The analysis period is from 2002 to 2019 and the grid resolution is 1.25° × 1.25° in the longitude–latitude directions. We used daily averages of the original 6-hourly data. Details of the data are described in Kobayashi et al. (2015). The Stratosphere-troposphere Processes And their Role in Climate (SPARC) Reanalysis Intercomparison Project (S-RIP) gives an evaluation of individual reanalysis datasets (Fujiwara et al., 2017).

2.2 Analysis methods

To analyze the wave-mean flow interaction, we consider planetary–scale waves based on the Transformed Eulerian Mean equations. We employed the Eliassen–Palm flux (E–P) to study the effect of the wave forcing on the zonal mean circulation. The vector of the E–P flux represents the direction of wave energy propagation in the zonal-mean circulation system. Moreover, the total wave forcing can be represented by the divergence (convergence) of the E–P flux, which is related to the acceleration (deceleration) of the westerly zonal-mean circulation (Andrews and McIntyre, 1976; Andrews et al., 1987). The E–P flux methodology in the quasi-geostrophic form is given by:

$$\boldsymbol{F} = \{F_y, F_z\} = \left\{-\rho a \cos\theta\, \overline{u'v'}, \rho a \cos\theta\, f \frac{\overline{v'\phi_z'}}{N^2}\right\} \quad (1)$$

where F_y and F_z represent the meridional and vertical components of the E–P flux, respectively. The zonal and meridional winds are denoted by u and v, respectively, and the prime denotes small perturbations to a steady zonal flow. The radius of the earth, the buoyancy frequency, density, latitude, vertical gradient of geopotential height, and the Coriolis parameter are represented by a, N, ρ, θ, ϕ_z, and f, respectively.

To study wave propagation, the distribution of the refractive index is analyzed based on

$$n_0^2 = \frac{\bar{q}_\phi}{a\bar{u}} - \frac{f^2}{4N^2H^2} \quad (2)$$

where n_0^2 is the squared refractive index; $\bar{q}_\phi$ is the meridional gradient of mean potential vorticity; $\bar{u}$ denotes a horizontal basic flow; and H is the scale height. For more details, see Andrews et al. (1987). Waves can propagate in regions of positive refractive index and are evanescent in the negative regions.

The present study investigates planetary-scale waves with zonal wavenumbers 1 to 3 by calculating the spatial Fourier transform in the longitudinal direction.

3 Results

https://doi.org/10.5194/acp-2021-444
Preprint. Discussion started: 1 July 2021

3.1 Overview of SSW2019

First, we present an overview of the SSW2019. Figure 1 shows the time-height cross-sections of the zonal-mean temperature gradient, ΔT, between 60°S and the South Pole, and the zonal-mean zonal winds at 60°S in 2019, and 2002 for comparison. In austral winter 2019, regular oscillations of ΔT occur in the upper stratosphere (~5 to 1 hPa) from June to the first half of July. In the SSW2002, intermittent warming of the South Pole first occurs in the upper stratosphere from mid-August, which is followed by a large warming in September. Except for a short warming period in the upper stratosphere in the middle of August 2019, the temperatures over the South Pole are lower than that at 60°S until late August. However, after a couple of warming pulses from late August to early September, the pronounced high temperature at the South Pole starts propagating downward to about 30 hPa from 19 September. After that, the warm conditions over the South Pole continue with regular warming pulses in the middle to the upper stratosphere (~20 to 1 hPa) until late October.

The zonal-mean zonal winds in the stratosphere are disturbed during SSW2019. From the beginning of June to late August, the zonal-mean zonal winds are regularly strengthened in the middle to the upper stratosphere (~20 to 1 hPa) with two maxima in late July and late August. In SSW2002, due to the regular oscillation of westerly winds in the middle to the upper stratosphere (~20 to 1 hPa), the PNJ is considerably weakened before the reversal of the zonal-mean zonal winds in September (see also Krüger et al., 2005). From late August to early September 2019, there are two substantial weakening periods of the PNJ from over 80 m s^{-1} to about 20 m s^{-1} in the upper stratosphere (~5 to 1 hPa), first from 26 August to 30 August and again from 1 September to 3 September (Figure 1). After the considerable deceleration of the westerly winds, a reversal of the zonal-mean zonal winds from westerlies to easterlies occurs in the middle of September above 5 hPa. Subsequently, there is another reversal to weak westerlies, lasting until the middle of October. Easterly winds occur again in the upper stratosphere (~5 to 1 hPa) after mid-October, leading to the gradual transition to the summer circulation. Since the reversal of zonal-mean zonal winds from westerlies to easterlies does not occur at 10 hPa and 60°S, SSW2019 is classified as a minor SSW.

3.2 Synoptic evolution

Figure 2 shows the synoptic evolution of temperature and geopotential height at 10 hPa on selected days in 2019. During the period 25–27 August, the cold polar vortex is located over the South Pole. It is partly surrounded by an anticyclone, with warm air on the edge of the polar vortex near southern Africa. From 28 August to 2 September, the warm air becomes warmer, whilst the low temperature region begins to push towards the South Pole. The anticyclone in the south of Australia begins to strengthen, corresponding to the amplified PW1. From 3–5 September, the temperatures decrease at the edge of the polar vortex while the vortex itself weakens further. The low temperature region is shifted off the centers of the vortices, indicating baroclinic conditions. Between 6 and 8 September, the high temperature stretches poleward, almost reaching the South Pole. The warming culminates on 11 September with a weakening of the polar vortex. The anticyclone also develops strongly during this period. After the peak warming, the warm air remains over the South Pole from 12 to 20 September and the anticyclone moves to the southwest of Australia.

https://doi.org/10.5194/acp-2021-444
Preprint. Discussion started: 1 July 2021

Atmospheric Chemistry and Physics Discussions

Figure 3a shows daily changes of zonal-mean temperatures at 90°S and 10 hPa from 1 June to 31 October. The temperatures in the middle stratosphere in high latitudes are higher than normal during the period from late August to September 2019 (red line). The climatological temperature (blue line) reaches its minimum around June and the interannual variability is relatively small at that time. After that, the temperature gradually increases and the interannual variability becomes larger, especially from September to October. In 2019, the temperature is close to the climatology until mid-August. Several warmings occur in late August, with pronounced warmings on 31 August 2019 and 11 September 2019. The temperature increase (ΔT) between 31 August and 11 September is ~40 K (hereafter referred to as the warming period). After the large temperature increase, a slight decrease occurs, but the high temperatures last for around one more week. Finally, the temperature attains a peak value of ~275 K on 19 September, which is about 10 days earlier than in 2002 (green line). The magnitude of the warming peak over the South Pole in September 2019 is well outside the standard deviation of the climatological temperature.

Figure 3b shows the zonal-mean zonal winds at 60°S and 10 hPa, where the wind speed exhibits near the peak of the PNJ maximum. The climatological zonal-mean zonal wind (blue line) peaks in August and decreases afterward, with large interannual variability. In 2019 (red line), the zonal-mean zonal wind changes by mid-August. A pronounced deceleration of the westerly winds to ~61 m s^{-1} occurs on 31 August, in accordance with the warming in late August. The westerly wind reaches a value of ~26 m s^{-1} on 11 September, coinciding with a warming peak in the temperature. The decrease in the magnitude of the wind (ΔU) is ~35 m s^{-1} from 31 August to 11 September 2019. The deceleration continues until mid-September, with the minimum westerly winds occurring on 17 September (~11 m s^{-1}). The magnitude of the weakening is ~50 m s^{-1} between 31 August and 17 September 2019. In 2002 (green line), the PNJ reverses to easterly winds on 27 September (~20 m s^{-1}), resulting in a difference of ~72 m s^{-1} from 24 August, when the first warming pulse occurs. Similar to the temperature evolution, the zonal-mean zonal wind is well outside the standard deviation of the climatology during September. However, there is no occurrence of the zonal-mean zonal wind reversal in 2019, which is one of the major differences compared with SSW2002.

3.3 Dynamical evolution

Figure 4 shows daily changes of the amplitudes of PW1 and PW2 in the geopotential height field ($Z_{1,2}$) at 60°S and 10 hPa (top) and the 50 hPa upward E–P fluxes for zonal wavenumbers 1–3 (bottom) in 2019 (left panels) and 2002 (right panels).

The quasi-stationary PW1 plays an important role in the dynamical evolution of SSW2019 (Fig. 4a). The largest Z_1 exceeded 2000 m on 8 September (~2137 m). Yamazaki et al. (2020) reported that this was the highest value of Z_1 that has been observed since August 2004 by Aura MLS in the SH. Large values of Z_1 also occurred from late August to the first half of September, which is consistent with the warming period. Another large amplification of Z_1 occurs in late August (Figure

https://doi.org/10.5194/acp-2021-444
Preprint. Discussion started: 1 July 2021

Atmospheric Chemistry and Physics
Discussions

4). These large amplifications of PW1 disturbed the polar vortex, leading to a weakening of the PNJ (Eswaraiah et al., 2020). The large growth of PW1 could be associated with the easterly phase of the quasi-biennial oscillation in the SH tropics (Eswaraiah et al., 2020; Rao et al., 2020). In comparison with the predominant role of PW1, PW2, and PW3 in SSW2002, Z_2 appears to be less dominant during the warming period from late August to the first half of September in SSW2019 (Figure 4). Furthermore, the eastward-traveling wave Z_2 presents around 31 July, 10 August, and 20 September 2019 at 10 hPa (not shown here), but is not as regular and pronounced as in 2002 (Krüger et al., 2005).

The vertical component of the E–P flux (hereafter EPFz) is a useful diagnostic for evaluating the vertical propagation of planetary waves into the stratosphere (e.g., Harada and Hirooka, 2017). Here we decompose the EPFz into contributions from zonal wavenumbers 1–3 to gain a deeper understanding of the wave activity during SSW2019 and SSW2002 in the stratosphere. In Fig. 4b, d, the daily evolution of the total EPFz at 50 hPa for all wavenumbers is shown by gray shading, along with the individual contributions from PW1–3 by colored lines. The total EPFz in 2019 indicates a high activity of planetary waves propagating into the stratosphere beginning in late August and attaining peak values in the first half of September, in accordance with the increasing temperatures at the South Pole and the weakening westerly winds. In addition, the contribution of zonal wavenumber 1 is considerably larger than the other zonal wavenumber components. However, the peak value of the total EPFz in 2019 does not surpass that in 2002. The SSW2019 is characterized by the large growth of PW1 activity that disturbed the polar vortex during the warming period.

Figure 5 shows the latitude-height cross-sections of zonal-mean zonal winds on several selected days. During the period 25–27 August, the westerly winds are located in the high latitudes of the stratosphere. As mentioned above, large-amplitude wave activity occurred from late August to the first half of September. The strength of the PNJ is considerably weakened from 28 to 30 September to about 65 m s^{-1} from a value exceeding 90 m s^{-1} between 25 and 27 August. Due to the large wave activity starting in late August, a substantial deceleration of the PNJ takes place from 28 August to 2 September. After a slight strengthening of the PNJ from 3 to 5 September, the PNJ weakens again and the core propagates downward during the period 6–11 September, in line with the large temperature increase observed in Figure 2. After the substantial deceleration of the PNJ, westerly winds remain relatively weak from 12 to 20 September and are characterized by a poleward shift of the westerly jet axis below 10 hPa. The deceleration of the PNJ from 12 to 20 September is in accordance with the warming over the South Pole observed in Figure 2.

We now examine the evolution of wave propagation from the troposphere to the stratosphere through the E–P flux. Figure 6 shows the time-height cross-sections of the E–P flux vectors and the divergence for PW1 and PW2 at 60°S. From Fig. 6a (PW1 during SSW2019), we see a pronounced upward propagation from the troposphere to the stratosphere and strong convergence of the E–P flux in the upper stratosphere in late August and the first half of September. In contrast to the large

https://doi.org/10.5194/acp-2021-444
Preprint. Discussion started: 1 July 2021

PW1 activity, the PW2 activity is fairly weak during the analysis period (Fig. 6b). This suggests that strong upward propagation of PW1 and strong convergence played an important role in triggering the SSW2019.

The planetary wave activity for SSW2002 has been well documented by Baldwin et al. (2003, their Fig. 6). Our Figure 6c, d confirms that both PW1 and PW2 periodically strengthens and propagates from the troposphere to the stratosphere. Strong convergence of the E–P flux appears intermittently in the upper stratosphere for both PW1 and PW2. This suggests that the PNJ and polar vortex were weakened by the intermittently strong wave activity, preconditioning the stratosphere before the occurrence of SSW2002 as mentioned earlier (Krüger et al., 2005). Subsequently, the polar vortex broke down due to the large wave activity in late September, which resulted in the reversal of the zonal-mean zonal wind at 60°S and 10 hPa, as shown in Figure 3b.

Figure 7 shows the latitude-height cross-sections of the E–P flux and the E–P flux divergence (convergence), which is related to the acceleration (deceleration) of the zonal-mean zonal winds, on the same selected days as for Figure 5. Pulses of strong wave forcing are observed in the stratosphere at high latitudes from late August to the first half of September 2019. From 28 to 30 August 2019, the waves strongly propagate upward and poleward from 60°S. Strong convergence is observed in the upper stratosphere, which corresponds to the strongly amplified planetary waves that lead to the deceleration of the PNJ mentioned above. From 31 August to 5 September, the waves propagate upward and equatorward, and the E–P flux converges in the upper stratosphere extratropic. During the period 6–8 September, a second maximum in the E–P flux convergence occurs, with wave propagation from the troposphere to the upper stratosphere at around 60°S. This convergence contributes to the occurrence of SSW2019 by decelerating the PNJ and warming the polar cap. Following this period of considerably large wave activity, regions of E–P flux convergence remain in the high latitudes around 10 hPa until 20 September. The long duration of E–P flux convergence corresponds to the continuously warming and weakening PNJ shown in Figures 2 and 5.

4 Discussion

We now discuss the mechanisms that generated the SSW2019.

In September 2019, the polar vortex is weakened mostly by strong PW1 forcing (Figures 2 and 4). To understand the wave-mean flow interaction with the acceleration (deceleration) of the zonal flow, we now consider the wave driving due to the divergence (convergence) of the E–P flux. Figure 8 shows the interannual variation in the divergence (convergence) of the E–P flux for PW1 and PW2 in September between 30°S and 90°S at 10 hPa from 2002 to 2019. Firstly, it is evident that the magnitude of the divergence of the E–P flux is larger in 2019 than in any other year within the past 18 years. In addition, this is predominantly driven by PW1. The magnitude of the divergence of the E–P flux in 2002 is the second largest within the analysis period. Here, we find that PW1, PW2, and PW3 all play an important role in SSW2002 (Figure 4). This is consistent with the study by Krüger et al. (2005).

https://doi.org/10.5194/acp-2021-444
Preprint. Discussion started: 1 July 2021

Atmospheric Chemistry and Physics
Discussions

One striking difference between the unusual major SSW2002 and minor SSW2019 in the SH is that the zonal-mean zonal winds did not reverse to easterly winds in 2019, as already mentioned above. Preconditioning is considered to be a characteristic of major SSWs (Labizke, 1981) and many studies have demonstrated the importance of preconditioning in SSW2002 (Allen et al., 2003; Baldwin et al., 2003; Newman and Nash, 2005). Krüger et al. (2005) highlighted the importance of the interaction of the eastward-traveling PW2 with the quasi-stationary PW1, which weakened the PNJ before the major SSW. For SSW2019, the planetary wave activity was not amplified (nor large) until late August. Moreover, compared with 2002, the eastward-traveling PW2 was less active and less pronounced before SSW2019 (not shown). In addition, the September SSW2019 occurred when the PNJ still had strong westerly winds. During SSW2019, westerly winds decreased by about 50 m s^{-1} from late August to the middle of September (see Figure 3). Despite the strong divergence of the E–P flux, it did not result in a reversal of the zonal-mean zonal winds at 10 hPa and below (Figure 8). However, similar or even smaller magnitudes of deceleration can result in a reversal of the zonal-mean zonal winds, as was observed for the major SSW in the NH winter of 2018/2019 (Rao et al., 2020). Here, the magnitude of weakening westerly winds could lead to major warming in the NH (Wargan et al., 2020).

The abrupt occurrence of wave propagation in the stratosphere played an important role in triggering SSW2019. As mentioned previously, strong upward planetary wave propagation took place from late August to the first half of September 2019. Here we offer a plausible mechanism underlying this phenomenon, namely that wave propagation from the troposphere to the stratosphere is controlled by the index of refraction, given that the refractive index and the meridional potential vorticity are highly correlated in the SH near the tropopause (Newman and Nash, 2005).

Figure 9 shows the meridional cross-sections of the refractive index before, during, and after SSW2019. From 28 August to 11 September 2019 (during the SSW2019), a wide waveguide (i.e., a positive refractive index) is formed from the troposphere to the stratosphere around 60°S. As planetary wave packets tend to propagate in regions with a large positive value of n_0^2, planetary waves propagate upward to the stratosphere through this waveguide. From 28 August to 11 September, there are high values of the refractive index in the high latitudes up to about 5 hPa. In addition, the strong PNJ before the SSW reduce from over 80 m s^{-1} to about 55 m s^{-1}. This is consistent with the strong wave propagation during the warming period shown in Figure 7. Some study suggests that planetary waves may propagate from the upper troposphere (see also Naoe et al., under review). After the pronounced warming occurred in late August to the first half of September, the persistent open waveguide in the high latitudes present until 20 September (after SSW2019). This allows the wave energy propagating from the troposphere to the stratosphere to continually weaken the PNJ.

5 Summary and Conclusion

In this study, the evolution of the Sudden Stratospheric Warming 2019 (SSW2019) in the Southern Hemisphere (SH) was analyzed using the JRA-55 meteorological reanalysis. An unusually large warming and decelerated westerly winds were

https://doi.org/10.5194/acp-2021-444
Preprint. Discussion started: 1 July 2021

observed in the southern polar region in September 2019. However, since a reversal from westerly winds to easterly winds did not take place at 60°S and 10 hPa, SSW2019 in the SH was classified as a minor SSW.

Temperatures increased strongly in the first part of September following a couple of abrupt warmings in late August. The temperatures at the South Pole were well below the climatological average and out of the standard deviation during most of September. The westerly winds decelerated abruptly in the stratosphere from late August. Although a reversal of zonal-mean zonal winds from westerlies to easterlies was observed in the upper stratosphere in early September, this reversal did not reach down to 10 hPa. In addition, the polar night jet (PNJ) was greatly weakened in the SSW2019.

The present study has shown that there was a pronounced amplification of the quasi-stationary planetary wave 1 (PW1) during SSW2019. The propagation of planetary waves to the stratosphere was investigated using the vertical component of the Eliassen–Palm (E–P) flux. High activity of planetary waves with a large contribution of PW1 propagated into the stratosphere at high latitude. Strong wave driving, represented by the convergence of the E–P flux, occurred in the upper stratosphere during the SSW2019, which led to the deceleration of the westerly winds. By studying the interannual variability of the wave forcing in September, we showed that the total wave forcing and the contribution from PW1 was larger in 2019 than in any other year during the analysis period (2002–2019).

The waveguide analysis showed that during the SSW2019, planetary waves propagated upward to the stratosphere through an open waveguide in the high latitudes. We found that a wide waveguide appeared at high latitudes from the lower to the upper stratosphere during SSW2019, which allowed planetary waves to propagate through the stratosphere. Moreover, because the waveguide existed after the pronounced warming, it allowed the planetary waves propagating upward to continually weaken the PNJ. This analysis revealed that strong and long-lasting quasi-stationary PW1 propagated to the stratosphere during the SSW2019. In contrast to the regular occurrence of the eastward-traveling PW2 during the SSW2002, the quasi-stationary PW1 played a dominant role in SSW2019.

The occurrence of preconditioning before the major warming in SSW2002 has been widely reported by many studies. However, similar preconditions were not found in SSW2019. This may be one of the reasons why the reversal of the zonal-mean zonal winds did not appear in SSW2019 at 10 hPa and below. Even though SSW2019 does not fulfil the criterion of a major SSW, the large increasing temperature at high latitudes still had a significant impact on the stratosphere, in particular on the formation of the Antarctic ozone hole in austral spring. Indeed, a diminished Antarctic ozone hole area has been observed in 2019.

Data availability

https://doi.org/10.5194/acp-2021-444
Preprint. Discussion started: 1 July 2021

Atmospheric Chemistry and Physics Discussions

The JRA-55 data set used in this paper is available on the JMA Data Dissemination System (https://jra.kishou.go.jp/JRA-55/index_en.html).

Author contribution

TH, NE, and KK designed the study, provided guidance and in the interpretation of the results, and reviewed the manuscript. GL performed the analysis and wrote the manuscript with contributions from TH, NE, and KK.

Competing interests

The authors declare that they have no conflicts of interest.

Acknowledgments

This study was partially supported by Grant-in-Aid for “2019 Initiative for Realizing Diversity in the Research Environment” through the “Diversity and Super Global Training Program for Female and Young Faculty (SENTAN-Q)”, Kyushu University from MEXT and by JSPS KAKENHI Grant numbers JP18H01280, JP18H01270, and JP20H01973. The GFD-DENNOU Library was used for graphical output.

https://doi.org/10.5194/acp-2021-444
Preprint. Discussion started: 1 July 2021

References

Al-Ajmi, D. N., Harwood, R. S. and Miles, T.: A sudden warming in the middle atmosphere of the southern hemisphere, Quart. J. Roy. Meteor. Soc., 111, 359-389, 1985.

Andrews, D. G. and McIntyre, M. E.: Planetary waves in horizontal and vertical shear: The generalized Eliassen-Palm relation and the mean zonal acceleration, J. Atmos. Sci., 33, 2031–2048, 1976.

Andrews, D. G., Holton, J. R., and Leovy, C. B.: Middle Atmosphere Dynamics, vol. 40 of International Geophysics Series, Academic Press, San Diego, USA, 1987.

Allen, D. R., Bevilacqua, R. M., Nedoluha, G. E., Randall, C. E., and Manney, G. L.: Unusual stratospheric transport and mixing during the 2002 Antarctic winter, Geophys. Res. Lett., 30, 1599, https://doi.org/10.1029/2003GL017117, 2003.

Baldwin, M. P., Ayarzagüena, B., Birner, T., Butchart, N., Butler, A. H., Charlton-Perez, A. J., Domeisen, D. I. V., Garfinkel, C. I., Garny, H., Gerber, E. P., Hegglin, M. I., Langematz, U., and Pedatella, N. M.: Sudden Stratospheric Warmings, Rev. Geophys., 59, e2020RG000708, https://doi.org/10.1029/2020RG000708, 2021.

Baldwin, M. P., Hirooka, T., O'Neill, T., and Yoden, S.: Major stratospheric warming in the Southern Hemisphere in 2002: Dynamical aspects of the ozone hole split, SPARC Newsletter, 20, 24–26, 2003.

Bancalá, S., Krüger, K., and Giorgetta, M.: The preconditioning of major sudden stratospheric warmings, J. Geophys. Res., 117, D04101, https://doi.org/10.1029/2011JD016769, 2012.

Barnett, J. J.: Large sudden warming in the southern hemisphere, Nature, 255, 387-389, 1974.

Charlton, A. J. and Polvani, L. M.: A new look at stratospheric sudden warmings. part i: Climatology and modeling benchmarks, J. Climate, 20, 449–469, https://doi.org/10.1175/JCLI3996.1, 2007.

Eswaraiah, S., Kim, J. -H., Lee, W., Hwang, J., Kumar, K. N., and Kim, Y. H.: Unusual Changes in the Antarctic Middle Atmosphere During the 2019 Warming in the Southern Hemisphere, Geophys. Res. Lett., https://doi.org/10.1029/2020GL089199, 2020.

Fujiwara, M., Wright, J. S., Manney, G. L., Gray, L. J., Anstey, J., Birner, T., Davis, S., Gerber, E. P., Harvey, V. L., Hegglin, M. I., Homeyer, C. R., Knox, J. A., Krüger, K., Lambert, A., Long, C. S., Martineau, P., Molod, A., Monge-Sanz, B. M., Santee, M. L., Tegtmeier, S., Chabrillat, S., Tan, D. G. H., Jackson, D. R., Polavarapu, S., Compo, G. P., Dragani, R., Ebisuzaki, W., Harada, Y., Kobayashi, C., McCarty, W., Onogi, K., Pawson, S., Simmons, A., Wargan, K., Whitaker, J. S., and Zou, C.-Z.: Introduction to the SPARC Reanalysis Intercomparison Project (S-RIP) and overview of the reanalysis systems, Atmos. Chem. Phys., 17, 1417–1452, https://doi.org/10.5194/acp-17-1417-2017, 2017.

Godson, W. L.: A comparison of middle-stratosphere behaviour in the Arctic and Antarctic, with special reference to final warmings, Proc. Int. Symp. on Stratospheric and Mesospheric Circulation, Berlin, Germany, 161-206, 1963.

https://doi.org/10.5194/acp-2021-444
Preprint. Discussion started: 1 July 2021

Atmospheric Chemistry and Physics Discussions

Harada, Y. and Hirooka, T.: Extraordinary features of the planetary wave propagation during the boreal winter 2013/2014 and the zonal wave number two predominance, J. Geophys. Res. -Atmos., 122, 11374-11387, https://doi.org/10.1002/2017JD027053, 2017.

Hendon, H. H., Thompson, D. W. J., Lim, E. P., Butler, A. H., Newman, P. A., Coy, L., Scaife, A., Polichtchouk, I., Garreaud, R. S., Shepherd, T. G., and Nakamura, H.: Rare forecasted climate event under way in the Southern Hemisphere, Nature, 573, 495–495, https://doi.org/10.1038/d41586-019-02858-0, 2019.

Hirota, I., Kuroi, K., and Shiotani, M.: Midwinter warmings in the Southern hemisphere stratosphere in 1988, Q. J. Roy. Meteor. Soc., 116, 929-941, 1990.

Iida, C., Hirooka, T., and Eguchi, N.: Circulation changes in the stratosphere and mesosphere during the stratospheric sudden warming event in January 2009, J. Geophys. Res. -Atmos., 119, 7104–7115, https://doi.org/10.1002/2013JD021252, 2014.

Julian, P. R.: Midwinter stratospheric warmings in the Southern Hemisphere: General remarks and a case study, J. Appl. Meteor., 6, 557–563, 1967.

Kobayashi, S., Ota, Y., Harada, Y., Ebita, A., Moriya, M., Onoda, H., Onogi, K., Kamahori, H., Kobayashi, C., Endo, H., Miyaoka, K., and Takahashi, K.: The JRA-55 Reanalysis: general specifications and basic characteristics, J. Meteorol. Soc. Jpn., 93, 5–48, https://doi.org/10.2151/jmsj.2015-001, 2015.

Krüger, K., Naujokat, B., and Labitzke, K.: The Unusual Midwinter Warming in the Southern Hemisphere Stratosphere 2002: A Comparison to Northern Hemisphere Phenomena, J. Atmos. Sci., 62, 603–613, https://doi.org/10.1175/JAS-3316.1, 2005.

Labitzke, K.: Midwinter warmings in the stratosphere and lower mesosphere, Zeitschr. Geophys., 34, 555–561, 1968.

Labitzke, K.: The amplification of height wave 1 in January 1979: A characteristic precondition for the major warming in February, Mon. Weather Rev., 109, 983-989, 1981.

Labitzke, K. and van Loon, H.: The stratosphere: phenomena, history, and relevance, Springer Verlag, Berlin, 197, 1999.

Labitzke, K. and van Loon, H.: A note on stratospheric midwinter warmings in the Southern Hemisphere, J. Appl. Meteor., 4, 292-295, 1965.

Matsuno, T.: A dynamical model of the stratospheric sudden warming, J. Atmos. Sci., 28, 1479–1494, 1971.

Naoe, H., Hirooka, T., Harada, Y., Kobayashi, C., Imada, Y., and Maeda, S.: Tropospheric Double-jet Structure related to a Pronounced Antarctic Stratospheric warming in September 2019, Geophys. Res. Lett., in review, 2020.

Naujokat, B. and Roscoe, H. K.: Evidence against an Antarctic stratospheric vortex split during the periods of pre-IGY temperature measurements, J. Atmos. Sci., 62, 885-889, 2005.

Newman, P. A. and Nash, E. R.: The Unusual Southern Hemisphere Stratosphere Winter of 2002, J. Atmos. Sci., 62, 614–628, https://doi.org/10.1175/JAS-3323.1, 2005.

Rao, J., Garfinkel, C. I., White, I. P., and Schwartz, C.: The Southern Hemisphere Minor Sudden Stratospheric Warming in September 2019 and its Predictions in S2S Models, J. Geophys. Res. -Atmos., 125, e2020JD032723, https://doi.org/10.1029/2020JD032723, 2020.

Roscoe, H. K., Shanklin, J. D., and Colwell, S. R.: Has the Antarctic vortex split before 2002?, J. Atmos. Sci., 62, 581–588, https://doi.org/10.1175/JAS-3331.1, 2005.

Safieddine, S., Bouillon, M., Paracho, A. C., Jumelet, J., Tencé, F., Pazmino, A., Goutail, F., Wespes, C., Bekki, S., Boynard, A., Hadji-Lazaro, J., Coheur, P. F., Hurtmans, D., and Clerbaux, C.: Antarctic Ozone Enhancement During the 2019 Sudden Stratospheric Warming Event, Geophys. Res. Lett., 47, e2020GL087810, https://doi.org/10.1029/2020gl087810, 2020.

Shiotani, M., Shimoda, N., and Hirota, I.: Inter-annual variability of the stratospheric circulation in the Southern Hemisphere, Q. J. R. Meteorol. Soc., 119, 531–546, 1993.

Stolarski, R. S., McPeters, R. D., and Newman, P. A.: The ozone hole of 2002 as measured by TOMS, J. Atmos. Sci., 62, 716–720, 2005.

Wargan, K., Weir, B., Manney, G. L., Cohn, S., and Livesey, N. J.: The anomalous 2019 Antarctic ozone hole in the GEOS Constituent Data Assimilation System with MLS observations, J. Geophys. Res.-Atmos., 125, e2020JD033335, https://doi.org/10.1029/2020JD033335, 2020.

Weber, M., Dhomse, S., Wittrock, F., Richter, A., Sinnhuber, B.-M., and Burrows, J. P.: Dynamical Control of NH and SH Winter/Spring Total Ozone from GOME Observations in 1995–2002, Geophys. Res. Lett., 30, 1853-1854, https://doi.org/10.1029/2002GL016799, 2003.

Yamazaki, Y., Matthias, V., Miyoshi, Y., Stolle, C., Siddiqui, T., Kervalishvili, G., Laštovička, J., Kozubek, M., Ward, W., Themens, D. R., Kristoffersen, S., and Alken, P.: September 2019 Antarctic sudden stratospheric warming: quasi-6-day wave burst and ionospheric effects, Geophys. Res. Lett., 47, e2019GL086577, https://doi.org/10.1029/2019GL086577, 2019.

https://doi.org/10.5194/acp-2021-444
Preprint. Discussion started: 1 July 2021

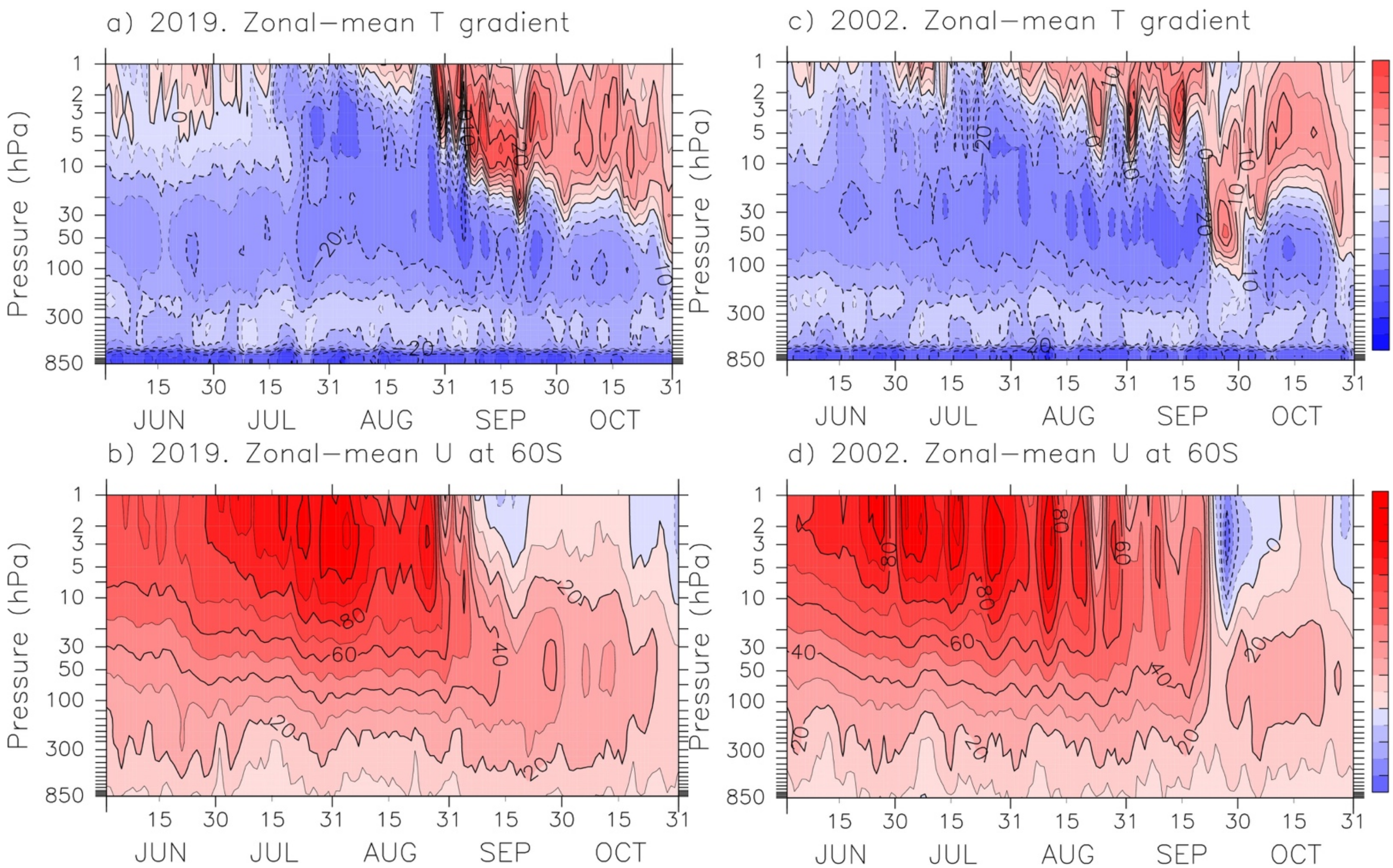

Figure 1. Time–height cross-sections of the temperature gradient [K] between 60°S and the South Pole (a,c) and the zonal-mean zonal wind [m s^{-1}] at 60°S (b,d) from 1 June to 31 October for 2019 (left) and 2002 (right). The contour intervals are 5 K for temperature and 10 m s^{-1} for zonal wind, respectively.

https://doi.org/10.5194/acp-2021-444
Preprint. Discussion started: 1 July 2021

Atmospheric Chemistry and Physics
Open Access
Discussions

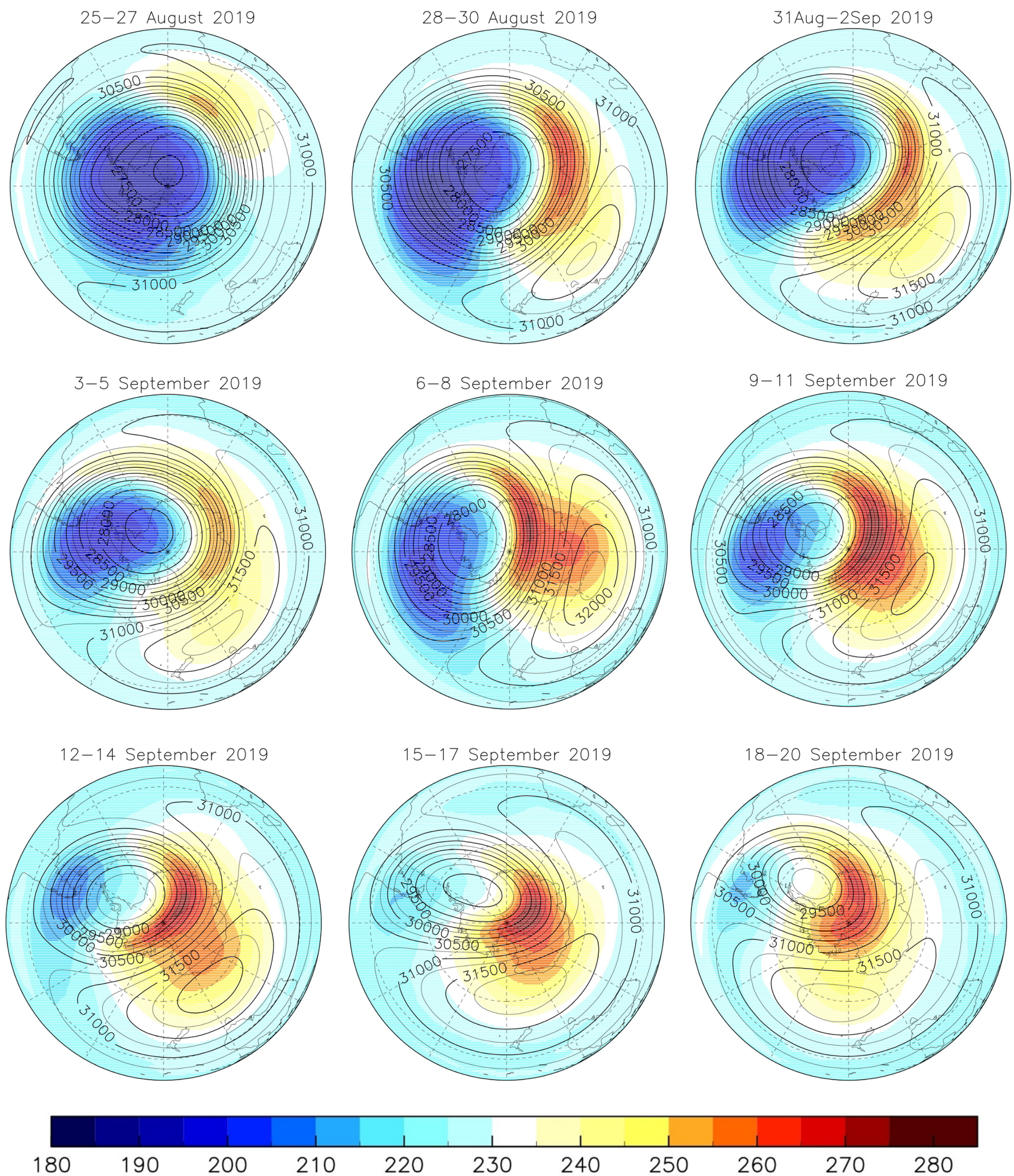

https://doi.org/10.5194/acp-2021-444
Preprint. Discussion started: 1 July 2021

Atmospheric Chemistry and Physics
Discussions

Figure 2. Polar stereographic map of temperatures [K] (colour shading) and geopotential heights [m] (contours) in the Southern Hemisphere at 10 hPa averaged every three days from 25 August to 20 September 2019. Contour intervals are 250 m.

https://doi.org/10.5194/acp-2021-444
Preprint. Discussion started: 1 July 2021

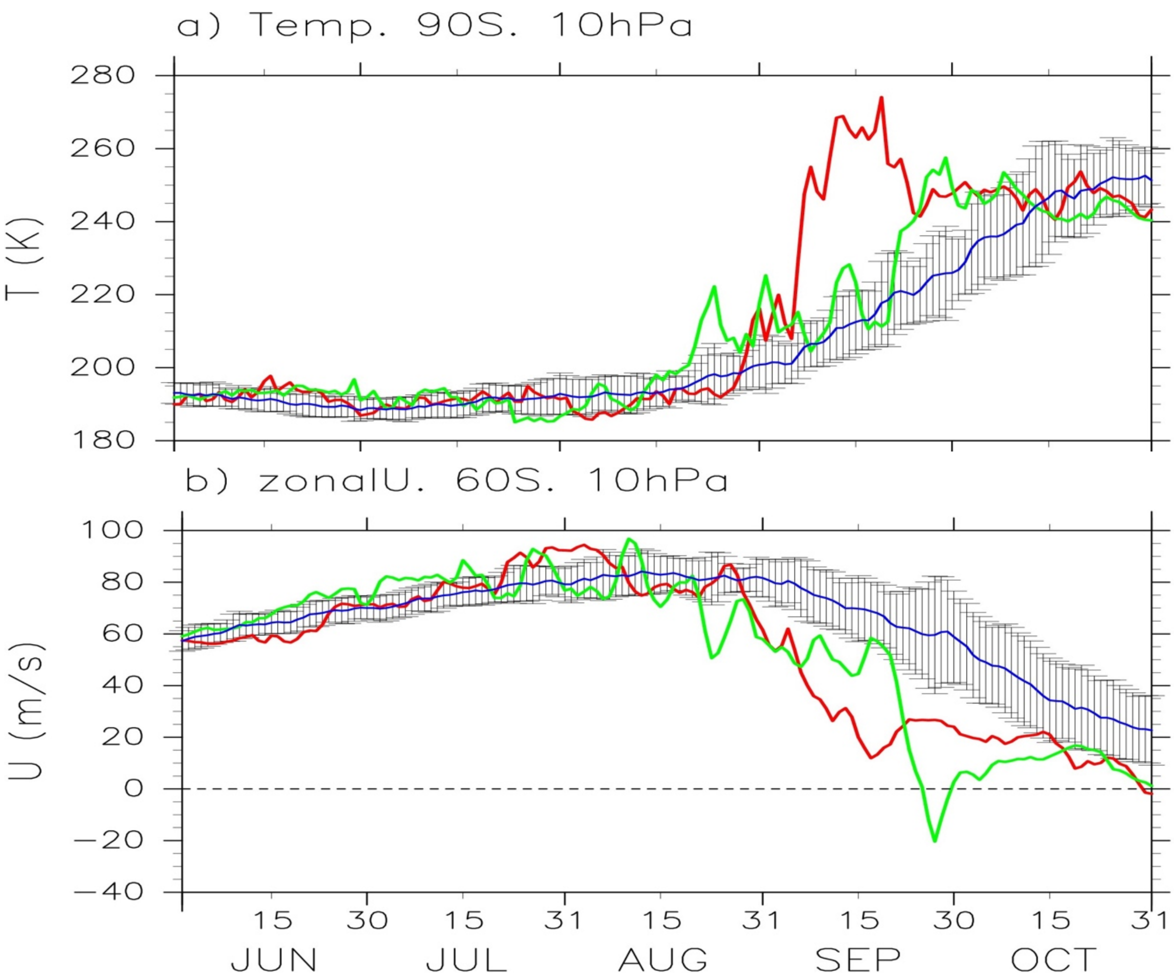

Figure 3. Time series of temperature [K] at 90°S and 10 hPa (a) and zonal-mean zonal wind [m s^{-1}] at 60°S and 10hPa (b) from 1 June to 31 October. Red and green lines show values for 2019 and 2002, respectively. Climatological values from 2002 to 2019 are represented by blue lines, with the standard deviation shown by error bars.

https://doi.org/10.5194/acp-2021-444
Preprint. Discussion started: 1 July 2021

Atmospheric Chemistry and Physics
Open Access
EGU
Discussions

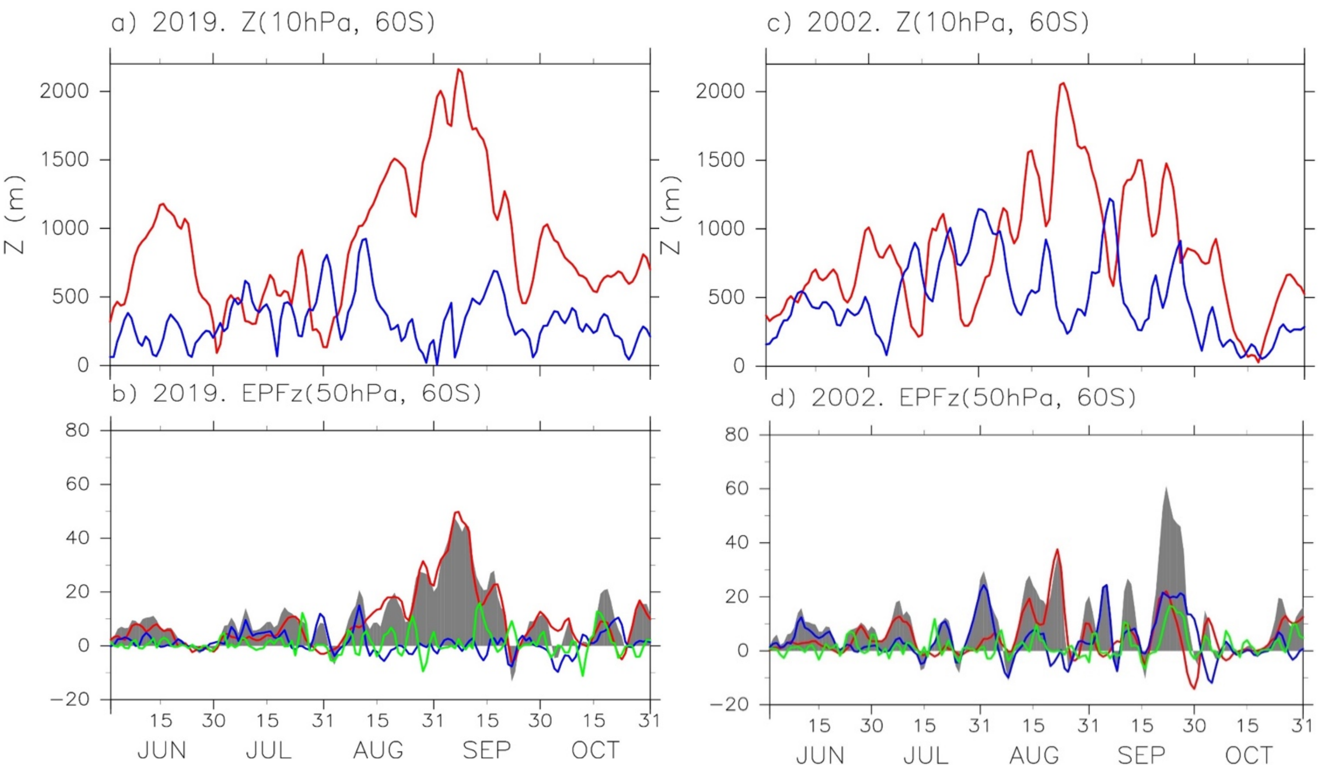

Figure 4. Time series of the amplitude [m] at 10 hPa and 60°S (a,c) and the vertical component of the E-P flux [$\times 10^4$ kg s^{-2}] at 60°S and 50 hPa (b,d) from 1 June to 31 October for 2019 (left) and 2002 (right). In the top panels, red and blue lines denote the zonal wavenumbers 1 and 2, respectively. In the bottom panels red, blue, and green lines denote the zonal wavenumbers 1, 2, and 3, respectively. Grey shadings show the vertical component of the E-P flux of all wavenumbers.

https://doi.org/10.5194/acp-2021-444
Preprint. Discussion started: 1 July 2021

Atmospheric Chemistry and Physics
Open Access
Discussions

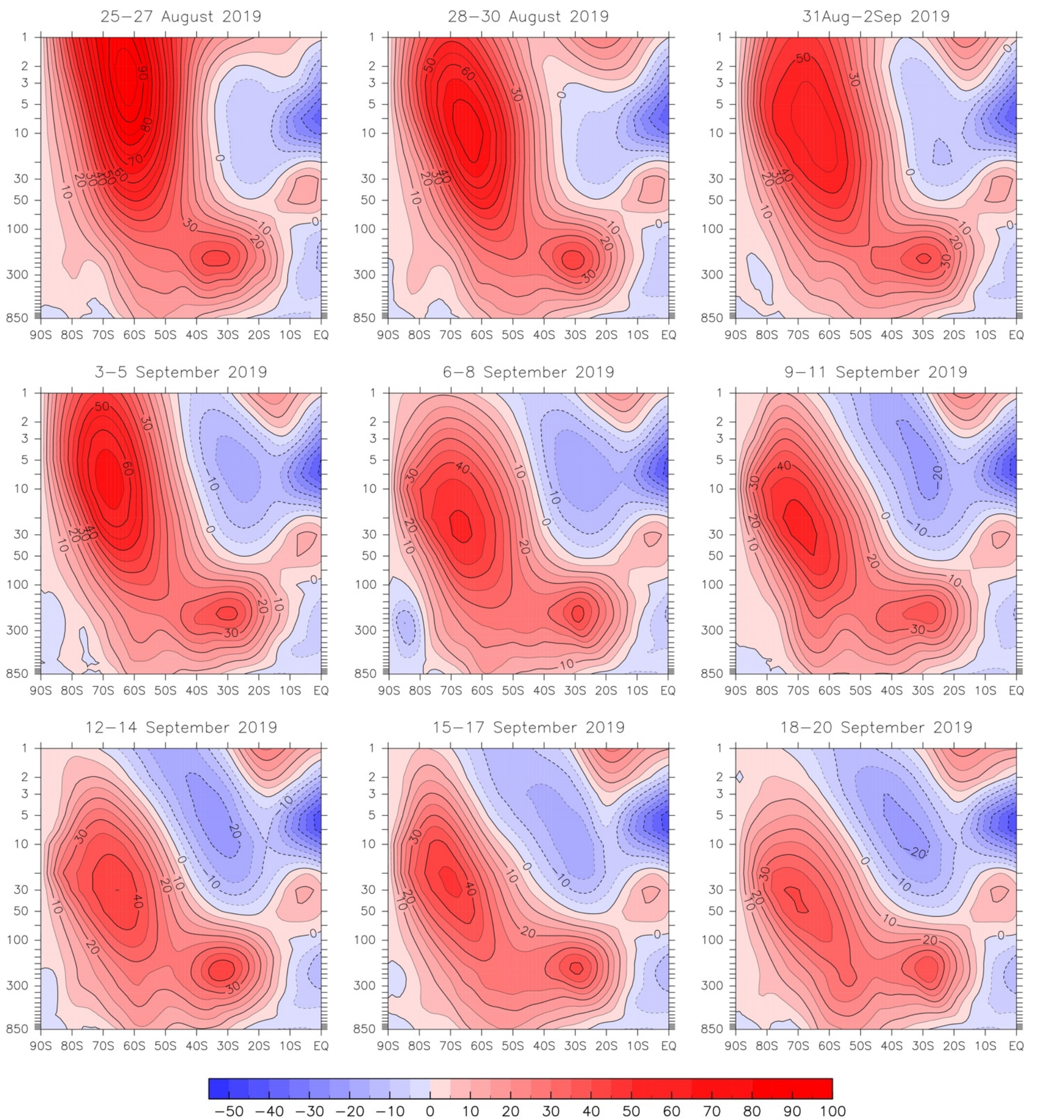

Figure 5. Latitude–height cross-sections of zonal-mean zonal wind [m s^{-1}] averaged every three days from 25 August to 20 September 2019. Contour intervals are 5 m s^{-1}.

https://doi.org/10.5194/acp-2021-444
Preprint. Discussion started: 1 July 2021

Atmospheric Chemistry and Physics Discussions
Open Access

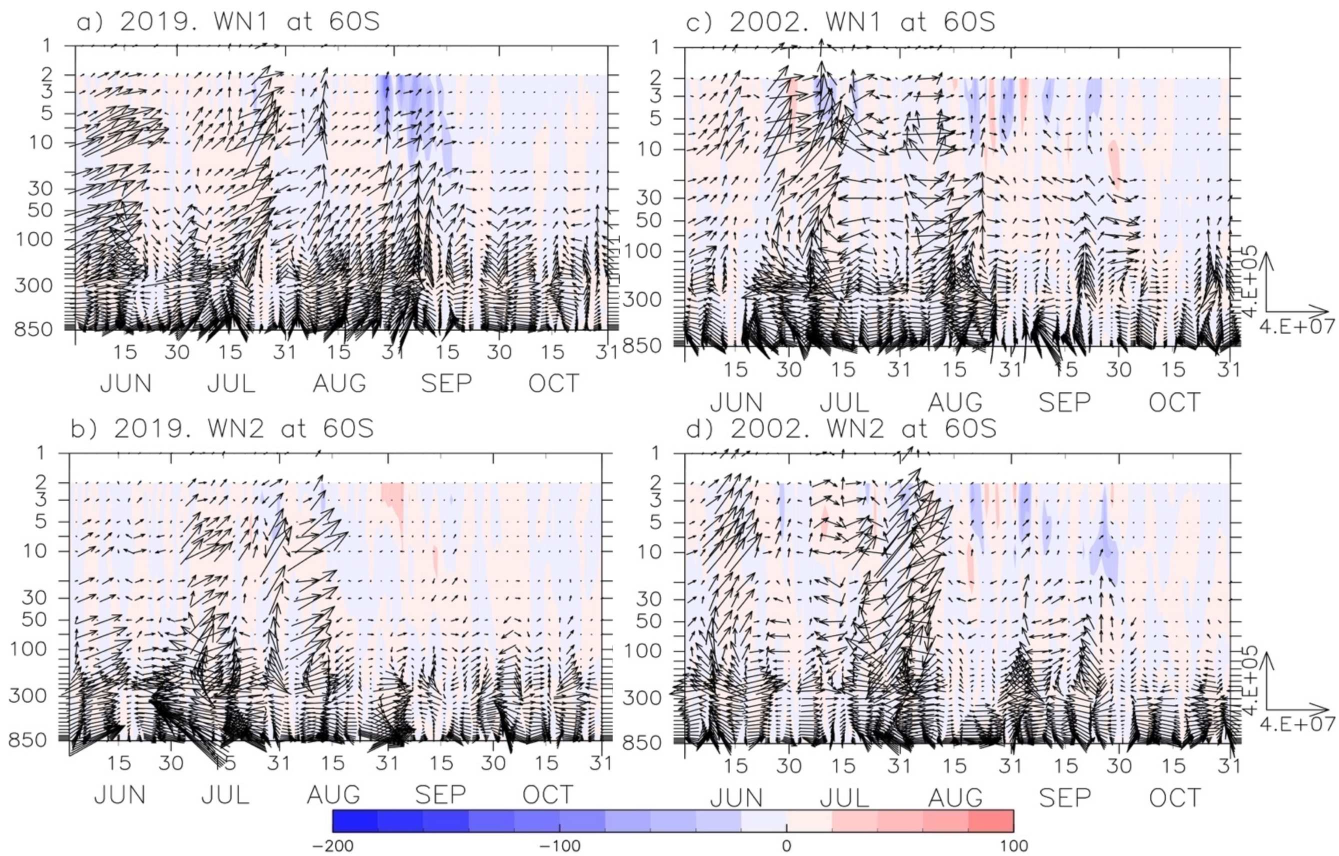

Figure 6. Time–height cross-sections of the E-P flux [kg s^{-2}] (vectors) at 60°S for zonal wavenumber 1 (a, c) and 2 (b, d) and the wave driving due to its divergence [m s^{-1} day^{-1}] (colour shading) from 1 June to 31 October in 2019 (left) and 2002 (right). E-P flux vectors pointing to the right direction corresponds to the poleward. The blue (red) shading denotes the zonal wind deceleration (acceleration).

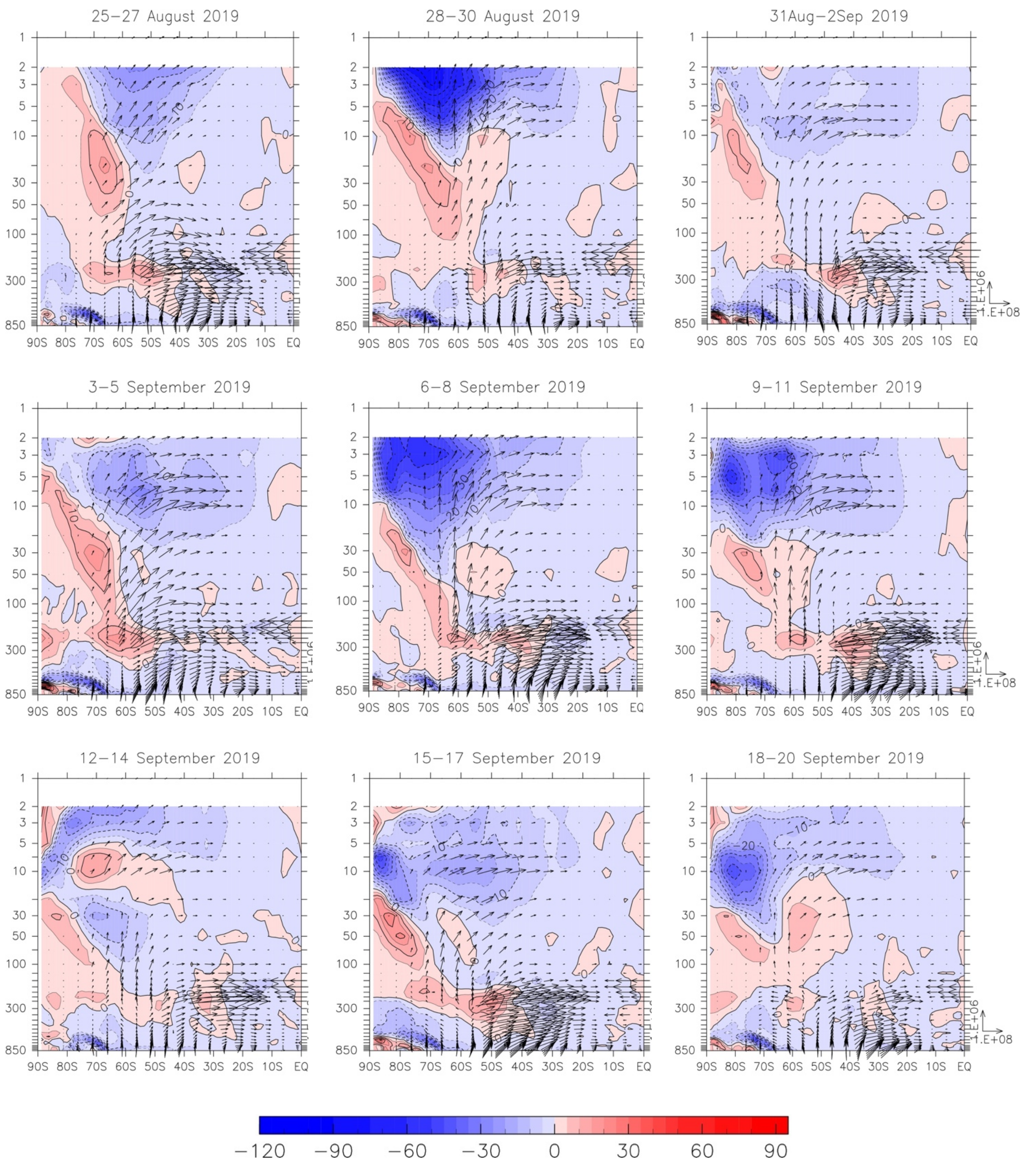

Figure 7. Same as Fig. 5 but for E-P flux [kg s^{-2}] (vectors) and the wave driving due to its divergence [m s^{-1} day^{-1}] (colour shading). Contour intervals are 5 m s^{-1} day^{-1}.

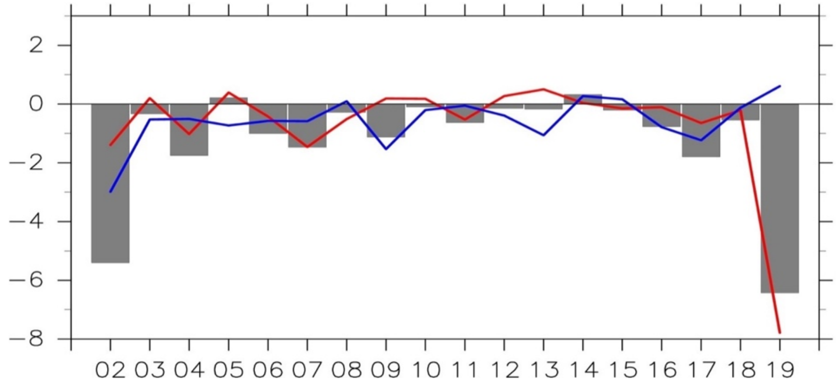

Figure 8. Interannual variations in wave driving due to E-P flux divergence [m s^{-1} day^{-1}] averaged over 30°-90°S at 10 hPa in September for zonal wavenumber 1 (red line) and 2 (blue line) from 2002 to 2019. Gray bars show the results for all wavenumbers.

https://doi.org/10.5194/acp-2021-444
Preprint. Discussion started: 1 July 2021

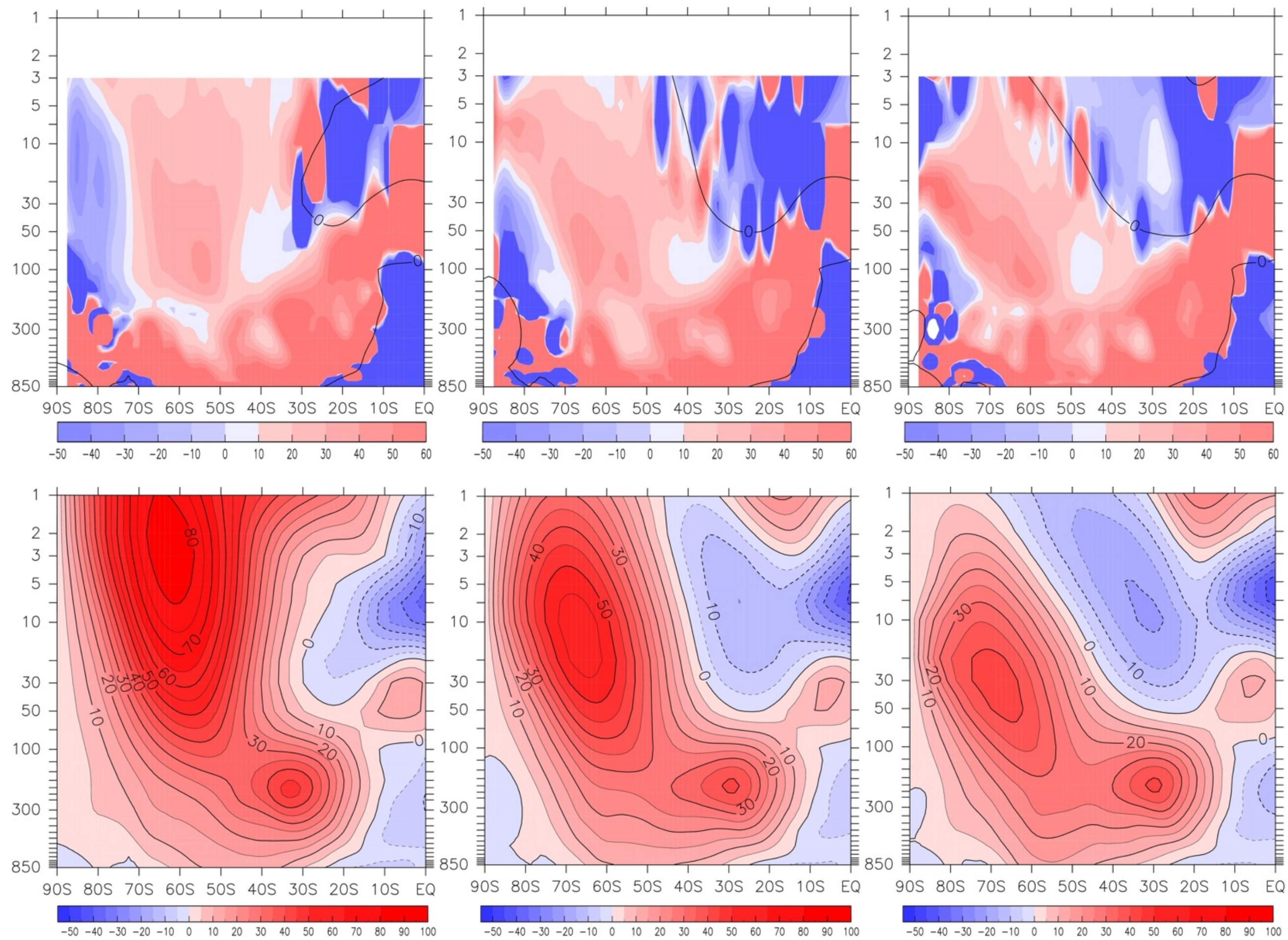

Figure 9. Same as Fig. 5 but for the quasi-geostrophic refractive index (dimensionless, colour shading, top) and zonal-mean zonal wind ([m s^{-1}], bottom) averaged over 10–20 August (left), 28 August–11 September (middle), and 12–20 September 2019 (right). Black lines in the top panels denote the zero-wind speed contour.